Molecular pathogenesis of esophageal squamous cell carcinoma: Identification of the antitumor effects of *miR-145-3p* on gene regulation

MASATAKA SHIMONOSONO[1*], TETSUYA IDICHI[1*], NAOHIKO SEKI[2], YASUTAKA YAMADA[2], TAKAYUKI ARAI[2], TAKAAKI ARIGAMI[1], KEN SASAKI[1], ITARU OMOTO[1], YASUTO UCHIKADO[1], YOSHIAKI KITA[1], HIROSHI KURAHARA[1], KOSEI MAEMURA[1] and SHOJI NATSUGOE[1]

[1]Department of Digestive Surgery, Breast and Thyroid Surgery, Graduate School of Medical Sciences, Kagoshima University, Kagoshima 890-8520; [2]Department of Functional Genomics, Chiba University Graduate School of Medicine, Chiba 260-8670, Japan

Received June 7, 2018; Accepted October 19, 2018

DOI: 10.3892/ijo.2018.4657

Abstract. Although *miR-145-5p* (the guide strand of the *miR-145* duplex) is established as a tumor suppressive microRNA (miRNA or miR), the functional significance of *miR-145-3p* (the passenger strand of the *miR-145* duplex) in cancer cells and its targets remains obscure. In our continuing analysis of esophageal squamous cell carcinoma (ESCC) pathogenesis, the aim of the present study was to identify important oncogenes and proteins that are controlled by *miR-145-3p*. Overexpression of *miR-145-3p* significantly reduced cancer cell proliferation, migration and invasive abilities, and further increased apoptotic abilities. In ESCC cells, 30 possible oncogenic targets were identified that might be regulated by *miR-145-3p*. Among these targets, dehydrogenase/reductase member 2 (*DHRS2*) and myosin IB (*MYO1B*) were focused on to investigate their functional roles in ESCC cells. *DHRS2* and *MYO1B* were directly regulated by *miR-145-3p* in ESCC cells by dual luciferase reporter assays. Aberrantly expressed *DHRS2* and *MYOIB* were detected in ESCC clinical specimens, and their overexpression enhanced cancer cell aggressiveness. Genes regulated by antitumor *miR-145-3p* were closely associated with the molecular pathogenesis of ESCC. The approach based on antitumor miRNAs may contribute to the understanding of ESCC molecular pathogenesis.

Correspondence to: Dr Naohiko Seki, Department of Functional Genomics, Chiba University Graduate School of Medicine, 1-8-1 Inohana, Chuo, Chiba 260-8670, Japan
E-mail: naoseki@faculty.chiba-u.jp

*Contributed equally

Key words: microRNA, passenger strand, microRNA-145-3p, esophageal squamous cell carcinoma, dehydrogenase/reductase member 2, myosin IB

Introduction

Esophageal squamous cell carcinoma (ESCC) is the most prevalent type of esophageal cancer and is the sixth leading cause of cancer mortality worldwide (1). Due to ESCC's aggressive nature, the prognosis of ESCC patients with local invasion and distant metastasis at diagnosis is poor (2,3). Surgical resection is recognized as the preferred treatment for patients with newly diagnosed ESCC. However, high rates of tumor recurrence are notable (4,5). Neoadjuvant chemotherapy or chemoradiotherapy have been demonstrated to prolong overall survival for patients with ESCC (6-8). However, treatment options for recurrent cases are limited, and recently approved targeted therapies have not observed effective therapeutic effects (9,10). Therefore, ESCC patients with recurrence and metastasis require novel and effective treatment strategies.

The latest genomic analyses of ESCC cells have exhibited epigenetic modifications, e.g., DNA methylation, histone deacetylation, chromatin remodeling and non-coding RNA regulation (11,12). In that regard, microRNAs (miRNAs or miRs) consist of a class of small, well-conserved, non-coding RNAs that regulate RNA transcripts in a sequence-dependent manner (13). They participate in physiological and pathological conditions, e.g., cell differentiation, proliferation, motility and metabolism (14). A single miRNA can control a vast number of RNA transcripts in normal and diseased cells (15). Therefore, aberrantly expressed miRNAs may break down regulated RNA networks and contribute to cancer cells' development, metastasis and drug resistance (16).

A large number of miRNAs exhibit differential expression in ESCC, and they contribute to ESCC pathogenesis through their activities as oncogenes or tumor suppressors (11). Analyses of our original miRNA expression signatures by RNA-sequencing revealed that both strands of the *miR-145* duplex (*miR-145-5p*, the guide strand and *miR-145-3p*, the passenger strand) were significantly downregulated in several types of cancers (17-20). The traditional view of miRNA function has held that only one strand of the miRNA duplex is incorporated into the RNA-induced silencing complex (RISC),

becoming the active strand (guide strand). In contrast, the other strand (the passenger strand or miRNA*) was thought to be degraded and to have no function (21,22). However, recent studies of miRNA biogenesis have demonstrated that certain miRNA passenger strands are functional in plant and human cells (20,23).

Our recent studies have demonstrated that both strands of the *miR-145* duplex have antitumor roles in lung cancer, bladder cancer, prostate cancer and head and neck cancer (17-20). In ESCC cells, both strands of the *miR-150* duplex (*miR-150-5p*, the guide strand, and *miR-150-3p*, the passenger strand) acted as antitumor miRNAs through their targeting of *SPOCK1* (24). A number of studies demonstrated that *miR-145-5p* acted as a pivotal antitumor miRNA in human cancers (25), including ESCC (26). In contrast, the functional significance and the targets of miR-145-3p are still obscure.

The aim of the present study was to demonstrate that *miR-145-3p* possesses antitumor functions and to identify its molecular targets, thereby elucidating ESCC pathogenesis. Thus, in ESCC cells, it was demonstrated that ectopic expression of *miR-145-3p* significantly blocked cancer cell proliferation, migration and invasion, similar to the actions of *miR-145-5p*. Furthermore, it was demonstrated that two genes, dehydrogenase/reductase member 2 (*DHRS2*) and myosin IB (*MYO1B*), were directly regulated by antitumor *miR-145-3p* in ESCC cells. Involvement of *miR-145-3p* (the passenger strand) is a novel concept in ESCC oncogenesis. The present approach, based on the roles of antitumor miRNA and its targets, will contribute to improved understanding of the molecular pathogenesis of ESCC.

Materials and methods

Human ESCC clinical specimens and cell lines. The present study was approved by the Bioethics Committee of Kagoshima University (Kagoshima, Japan; approval no. 28-65). Written prior informed consent and approval were obtained from all of the patients. All subjects in the patient cohort (n=29) were diagnosed with ESCC based upon pathologic criteria. ESCC with curative resection was included, salvage surgery was excluded. From this group, 22 clinical specimens and 12 noncancerous esophageal tissues were obtained. All samples were collected at the Kagoshima University hospital from March 2010 to September 2014. Collection of resected tissues occurred prior to preoperative therapy. The clinicopathological features of the patients are presented in Tables I and II. ESCC is more prevalent among males, thus almost all cases recruited for the present study were male.

In addition, 2 ESCC cell lines were used: TE-8, moderately differentiated and TE-9, poorly differentiated (27) (RIKEN BioResource Center, Tsukuba, Japan). Cell culture, extraction of total RNA and extraction of protein were performed as described in previous reports (28,29).

Transfection of mimic and inhibitor miRNA, small interfering (si)RNA into ESCC cells. In the present study, the following mimic and inhibitor miRNAs or siRNAs were transfected: mimic miRNAs (Ambion Pre-miR miRNA precursor; *miR-145-5p*: 5'-GUCCAGUUUUCCCAGGAAUCCCU-3', ID: PM11480; *hsa-miR-145-3p*: 5'-GGAUUCCUGGAAAUACUGUUCU-3', ID: PM13036; Thermo Fisher Scientific, Inc., Waltham, MA, USA), inhibitor miRNAs (Anti-miR miRNA Inhibitor; *has-miR-145-3p*: 5'-GGAUUCCUGGAAAUACUGUUCU-3', ID: AM13036; Applied Biosystems; Thermo Fisher Scientific, Inc.) and siRNAs (Stealth Select RNAi siRNA; si-*DHRS2*, ID: HSS145497 and HSS173461; si-*MYO1B*, ID: HSS106714 and HSS106716; Invitrogen; Thermo Fisher Scientific, Inc.) and negative control miRNA/siRNA (product ID: AM17111; Thermo Fisher Scientific, Inc.). The transfection procedures were performed as previously described (28-30).

Incorporation of miR-145-3p into the RISC: Assessment by argonaute 2 (Ago2) immunoprecipitation. miRNAs were transfected into TE-8 cells and miRNAs were isolated using an microRNA Isolation Kit, Human Ago2 (Wako Pure Chemical Industries, Ltd., Osaka, Japan) as described previously (28-30). The expression levels of Ago2-conjugated miRNAs were assessed by reverse transcription-quantitative polymerase chain reaction (RT-qPCR). miR-21 (assay ID; 000397; Applied Biosystems) was used as the internal control.

RT-qPCR. Quantification of miRNAs and mRNAs was performed by StepOnePlus™ Real-Time PCR System (Thermo Fisher Scientific, Inc.). The procedure used for RT-qPCR has been described previously (28,29). The expression levels of miRNAs were analyzed using TaqMan RT-qPCR assays (*miR-145-5p*, assay ID: 002278; *miR-145-3p* assay ID: 002149; Applied Biosystems; Thermo Fisher Scientific, Inc.). Data were normalized to *RNU48* (assay ID: 001006; Applied Biosystems). In addition, the expression levels of *DHRS2* and *MYO1B* were assessed with the following TaqMan probes: *DHRS2*, assay ID: Hs01061575_g1; *MYO1B*, assay ID: Hs00362654_m1; Applied Biosystems; Thermo Fisher Scientific, Inc.), and normalized to glucuronidase β (assay ID: Hs00939627_ml; Applied Biosystems; Thermo Fisher Scientific, Inc.).

Cell proliferation, migration, invasion and apoptosis assays. Protocols for determining cell proliferation (XTT assays), migration and invasion were described previously (28,29). For apoptosis assays, double staining with fluorescein isothiocyanate (FITC)-Annexin V and propidium iodide was carried out using a FITC Annexin V Apoptosis Detection kit (BD Biosciences, Franklin Lakes, NJ, USA) according to the manufacturer's recommendations. Stains were analyzed within 1 h using a flow cytometer (CyAn ADP analyzer; Beckman Coulter, Inc., Brea, CA, USA). Cells were identified as viable cells, dead cells, early apoptotic cells and late apoptotic cells using Summit 4.3 software (Beckman Coulter, Inc.). The percentages of early apoptotic and late apoptotic cells from each experiment were then compared. As a positive control, 1 μM gemcitabine hydrochloride (Tokyo Chemical Industry Co., Ltd., Tokyo, Japan) was used.

Identification of putative target genes regulated by miR-145-3p in ESCC cells. The present strategy for identification of miR-145-3p target genes is outlined in Fig. 1. The microarray data were deposited in the Gene Expression Omnibus (GEO) repository (https://www.ncbi.nlm.nih.gov/geo/) under accession number GSE107008. Putative target genes with a binding site for *miR-145-3p* were detected by TargetScanHuman ver.7.1

Table I. Clinicopathological features of esophageal squamous cell carcinoma patients.

No.	Age (years)	Sex	Differentiation	T	N	M	Stage	ly	v	Recurrence
1	52	Male	Poor	1b	0	0	IA	1	1	+
2	72	Male	Moderate	1b	0	0	IA	0	1	-
3	69	Male	Moderate	1b	0	0	IA	0	0	-
4	56	Male	Moderate	2	0	0	IB	0	1	-
5	66	Male	Moderate	3	0	0	IIA	1	1	-
6	70	Male	Moderate	3	0	0	IIA	1	1	+
7	66	Male	Moderate	3	0	0	IIA	1	1	-
8	71	Male	Well	3	0	0	IIA	1	2	-
9	62	Male	Well	1a	1	0	IIB	0	0	-
10	68	Male	Moderate	1b	1	0	IIB	1	1	-
11	60	Male	Moderate	1b	1	0	IIB	1	1	-
12	71	Male	Moderate	1b	1	0	IIB	0	0	-
13	84	Male	Well	2	1	0	IIB	1	1	-
14	79	Male	Moderate	2	1	0	IIB	1	1	-
15	60	Male	Moderate	2	1	0	IIB	1	2	-
16	68	Male	Poor	1b	2	0	IIIA	1	3	+
17	67	Male	Well	3	2	0	IIIB	2	2	+
18	55	Male	Moderate	3	2	0	IIIB	1	1	+
19	75	Male	Moderate	3	2	0	IIIB	1	1	+
20	74	Male	Moderate	2	3	0	IIIC	3	1	+
21	57	Male	Poor	3	3	0	IIIC	1	1	+
22	63	Male	Well	3	3	0	IIIC	2	1	+

ly, lymphatic invasion; M, metastasis; N, nodes; T, tumor; v, venous invasion.

Table II. Features of patients in noncancerous esophageal tissues.

No.	Age (years)	Sex
1	66	Male
2	55	Male
3	52	Male
4	78	Male
5	75	Male
6	60	Male
7	71	Male
8	64	Male
9	79	Female
10	81	Male
11	69	Male
12	84	Male

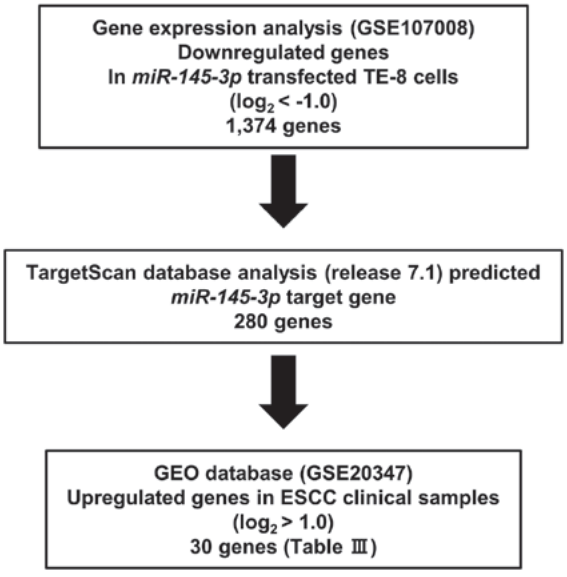

Figure 1. Strategy for identification of putative target genes regulated by *miR-145-3p* in ESCC cells. Gene expression analyses demonstrated that 1,374 genes were downregulated in *miR-145-3p*-transfected TE-8 cells. Finally, 30 genes were selected as putative targets of *miR-145-3p* in ESCC cells. miR, microRNA; ESCC, esophageal squamous cell carcinoma.

(http://www.targetscan.org/vert_71/). The GEO database (GSE20347) was used for assessment of the association between target genes and ESCC.

Exploration of downstream targets regulated by si-DHRS2 and si-MYO1B in ESCC. Genome-wide microarray analysis was used for identification of *DHRS2* and *MYO1B* downstream targets. Expression data were deposited in a GEO database (GSE118966). A GEO database (GSE20347) was used for assessment of the association between target

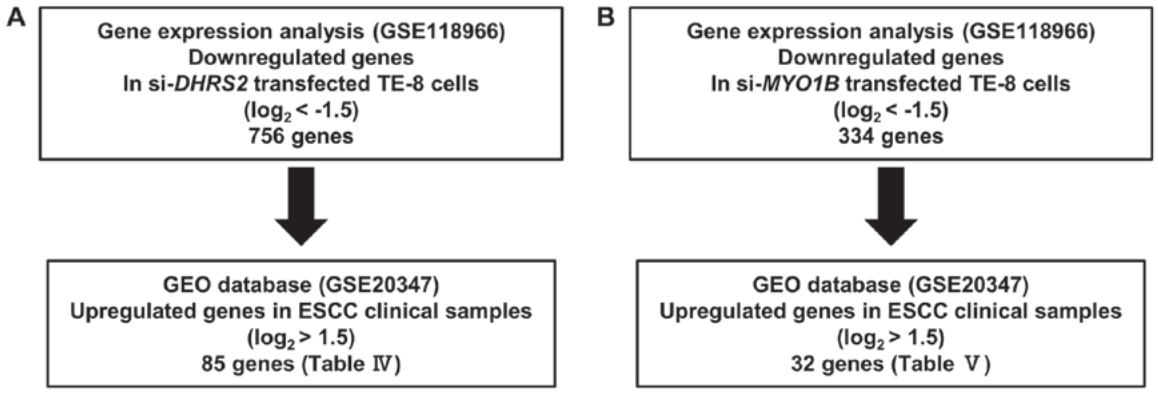

Figure 2. Strategy for identification of putative downstream genes regulated by (A) si-*DHRS2* and (B) si-*MYO1B* in TE-8 cells. Microarray analyses were performed using TE-8 cells in which *DHRS2* or *MYO1B* were knocked down to identify candidate genes that were downstream. si, small interfering RNA; DHRS2, dehydrogenase/reductase member 2; MYO1B, myosin IB.

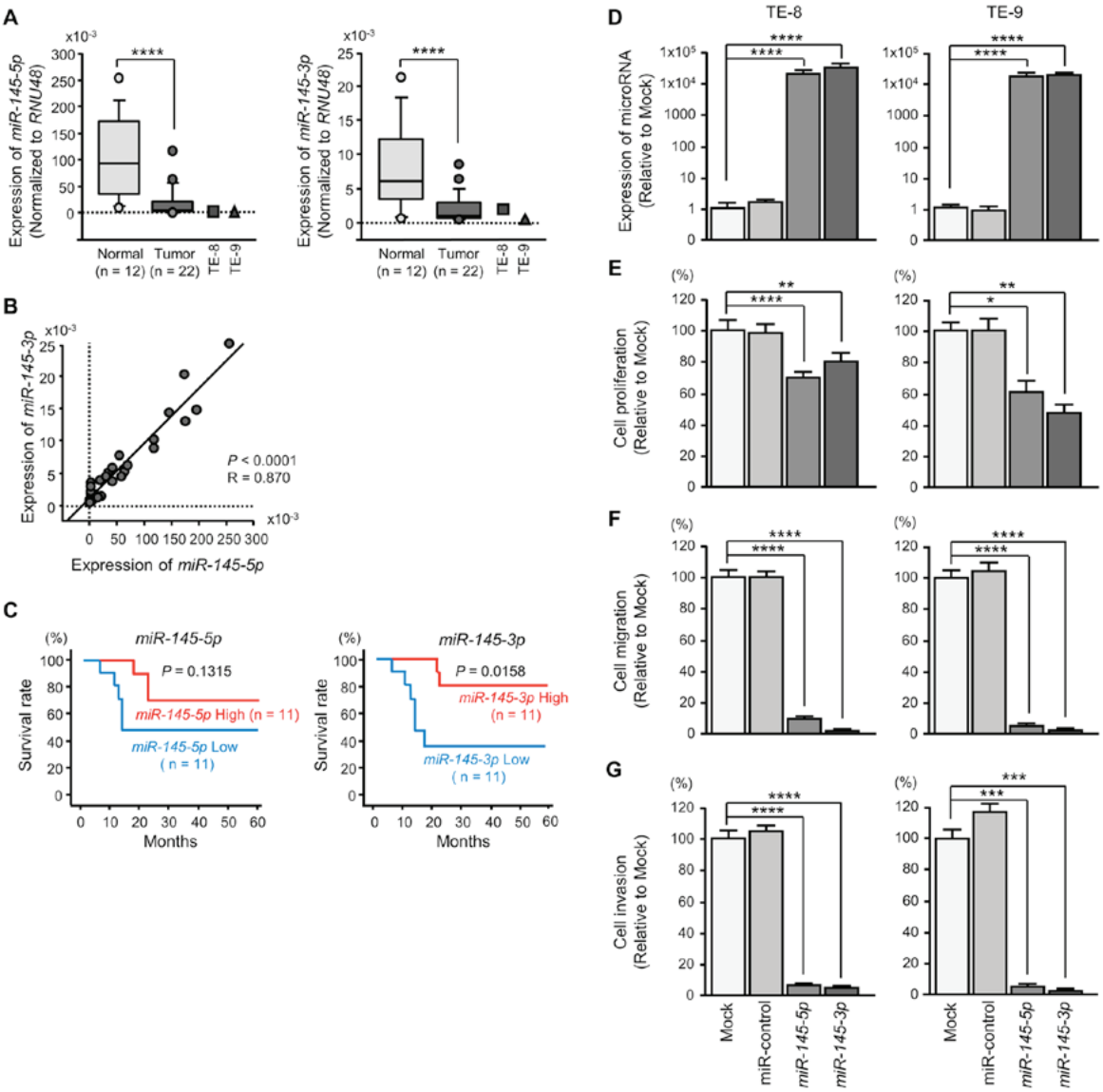

Figure 3. Effects of ectopic expression of *miR-145-5p* and *miR-145-3p* on ESCC cells. (A) Expression levels of *miR-145-5p* and *miR-145-3p* in ESCC clinical specimens and cell lines. *RNU48* was used as an internal control. (B) Spearman's rank test demonstrated a positive correlation between the expression levels of *miR-145-5p* and *miR-145-3p*. (C) The 5-year survival rates were analyzed by Kaplan-Meier survival curves and log-rank statistics. (D) Expression levels of *miR-145-5p* and *miR-143-3p* in ESCC cell lines. RNU48 was used as an internal control. TE-8 and TE-9 cells were transfected for 72 h following transfection with 10 nM *miR-145-5p* and *miR-143-3p* mimic. (E) Cell proliferation was determined by XTT assays 72 h following transfection with *miR-145-5p* and *miR-145-3p*. (F) Results of cell migration assays. (G) Cell invasion activity was determined using Matrigel invasion assays. *P<0.05, **P<0.01, ***P<0.001, ****P<0.0001. miR, microRNA; ESCC, esophageal squamous cell carcinoma.

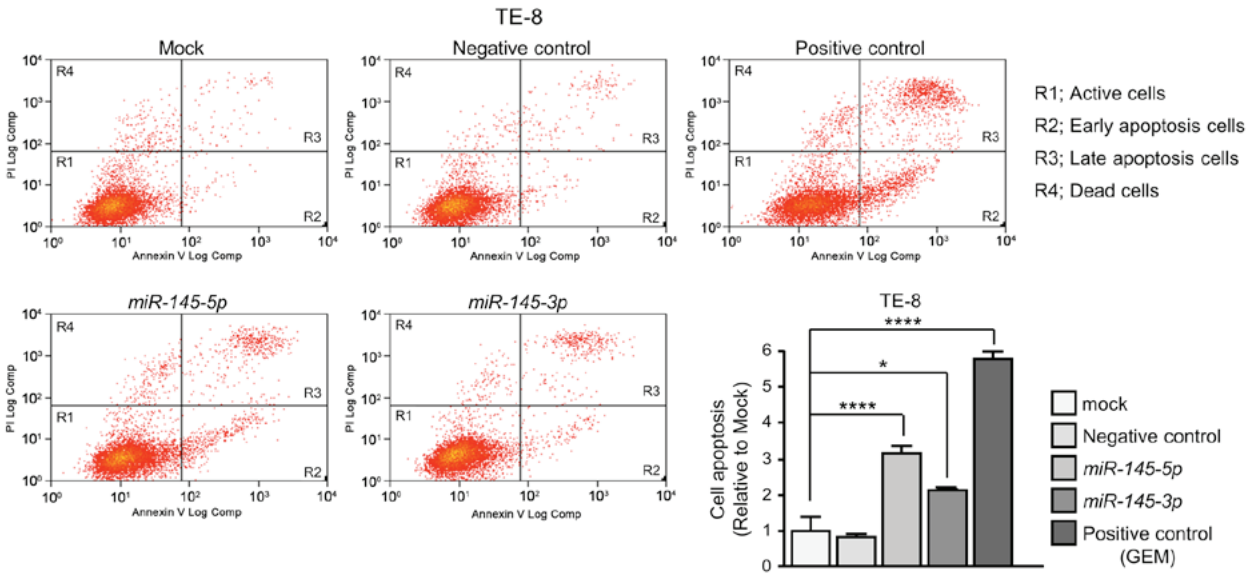

Figure 4. Effects of *miR-145-5p* and *miR-145-3p* on TE-8 cell apoptosis. Apoptosis assays were performed using a fluorescein isothiocyanate Annexin V apoptosis detection kit with flow cytometric determination. Early apoptotic cells are in area R2 and late apoptotic cells are in area R3. The normalized ratios of early and late apoptotic cells are presented in the histogram. GEM was used as a positive control. *P<0.05, ****P<0.0001. miR, microRNA; GEM, gemcitabine hydrochloride.

genes and ESCC. Our strategy for identification of *DHRS2* and *MYO1B* downstream targets is outlined in Fig. 2. Expression analysis was performed on microarray data using SurePrint G3 Human 8x60K v3 (Agilent Technologies, Inc., Santa Clara, CA, USA).

Western blot analysis. Anti-human DHRS2 rabbit polyclonal immunoglobulin (Ig)G (1:1,000; HPA069551; Sigma-Aldrich; Merck KGaA) and anti-human MYO1B rabbit polyclonal IgG (1:250; HPA013607; Sigma-Aldrich; Merck KGaA) were used as primary antibodies. Anti-human β-actin mouse monoclonal IgG (1:2,000; A1978; Sigma-Aldrich; Merck KGaA) was used as an internal control. The protocol for Western blot analysis was described previously (29,30).

Immunohistochemistry. Tumor specimens were fixed, embedded and sectioned as described previously (31). Anti-human DHRS2 rabbit polyclonal IgG (1:250; HPA069551; Sigma-Aldrich, St. Louis, MO, USA) and anti-human MYO1B rabbit polyclonal IgG (1:300; HPA013607; Sigma-Aldrich; Merck KGaA were used as primary antibodies. The protocol followed was described previously (32).

Luciferase reporter assays. The following sequences were inserted into the psiCHECk-2 vector (C8021; Promega Corporation, Madison, WI, USA): The wild-type sequences of the 3'-untranslated regions (UTRs) of *DHRS2* and *MYO1B*, or the deletion-type, which lacks the miR-145-3p target sites from *DHRS2* (position 270-276) or *MYO1B* (position 88-94 or position 1,117-1,123). The cloned vectors were co-transfected into ESCC cells with mature *miR-145-3p*. The procedures for transfection and dual-luciferase reporter assays have been reported previously (28,29).

Statistical analysis. Associations between groups were analyzed using the Mann-Whitney U test or Tukey's multiple comparisons test following one-way analysis of variance. The differences between survival rates were analyzed by Kaplan-Meier survival curves and log-rank statistics. Spearman's rank test was used to evaluate the correlations between the expression levels of *miR-145-3p*, *miR-145-5p*, *DHRS2* and *MYO1B*. Data are presented as the mean ± standard deviation. P<0.05 was considered to indicate a statistically significant difference. Expert StatView version 5.0 (SAS Institute, Inc., Cary, NC, USA) and GraphPad Prism version 7.04 (GraphPad Software, Inc., La Jolla, CA, USA) were used in these analyses.

Results

Expression levels of miR-145-5p and miR-145-3p in ESCC clinical specimens. Expression levels of *miR-145-5p* and *miR-145-3p* were significantly downregulated in cancer tissues and ESCC cell lines relative to normal tissues (Fig. 3A). Spearman's rank test demonstrated a positive correlation between the expression levels of *miR-145-5p* and *miR-145-3p* (Fig. 3B).

It was demonstrated that 5-year survival was significantly higher in patients who had high *miR-145-3p* expression than in patients with low *miR-145-3p* expression (Fig. 3C). There was no significant association between the expression level of *miR-145-5p* and patient survivals (Fig. 3C).

Ectopic expression of miR-145-5p and miR-145-3p: Impact on ESCC cells. To assess the ectopic expression of *miR-145-5p* and *miR-145-3p*, the mimic miRNA was transfected to ESCC cell lines (Fig. 3D). XTT assays demonstrated significant inhibition of cell proliferation in *miR-145-5p* and *miR-145-3p* transfectants (Fig. 3E). Likewise, cell migration and invasion were significantly inhibited following miR-145-5p or *miR-145-3p* transfection (Fig. 3F and G). The numbers of early apoptotic and late apoptotic cells were significantly larger in

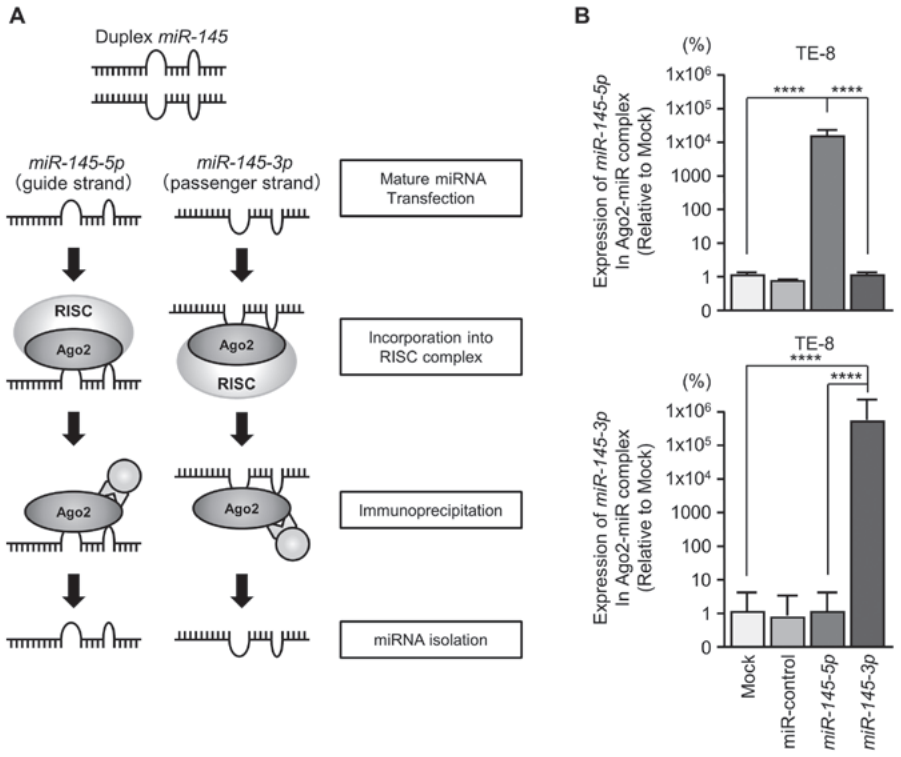

Figure 5. Both strands of *miR-145* duplex bound to Ago2. (A) Schematic illustration of miRNA detection methods. Isolation of RISC incorporated miRNAs by Ago2 immunoprecipitation. (B) Expression levels of miRNAs bound to Ago2 were assessed by reverse transcription-quantitative polymerase chain reaction. Expression data were normalized by the expression of *miR-21*. ****P<0.0001. miR/miRNA, microRNA; Ago2, argonaute 2; RISC, RNA-induced silencing complex.

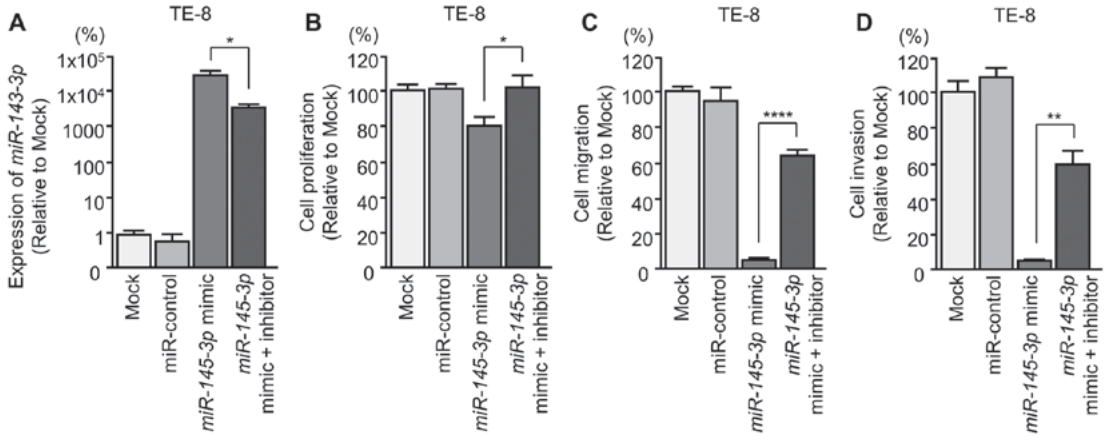

Figure 6. Rescue experiments: Tumor suppressive effect of *miR-145-3p* by mimic and inhibitor using ESCC cells. TE-8 cells were transfected with 10 nM *miR-145-3p* mimic to overexpress *miR-145-3p*; the tumor suppressive effects of TE-8 were readily observed. However, co-transfection of 10 nM *miR-145-3p* mimic and inhibitor demonstrated that the tumor suppressive effects of *miR-145-3p* were attenuated. (A) Expression levels of *miR-145-3p* in ESCC cell lines. *RNU48* was used as an internal control. TE-8 cells were transfected for 72 h following co-transfection with 10 nM *miR-145-3p* mimic and inhibitor. (B) Cell proliferation activity was assessed by XTT assays. TE-8 cells were transfected for 72 h following co-transfection with 10 nM *miR-145-3p* mimic and inhibitor. (C) Cell migration activity was assessed 72 h following co-transfection with 10 nM *miR-145-3p* mimic and inhibitor. (D) Cell invasion activity was determined using Matrigel 72 h following co-transfection with 10 nM *miR-145-3p* mimic and inhibitor. *P<0.05, **P<0.01, ****P<0.0001. miR, microRNA; ESCC, esophageal squamous cell carcinoma.

miR-145-5p or *miR-145-3p* transfectants than in mock or negative control transfectants (Fig. 4).

Incorporation of miR-145-3p into the RISC in ESCC cells. It was anticipated that the passenger strand of *miR-145-3p* was incorporated into the RISC and served as a tumor suppressor in ESCC cells. To verify that hypothesis, Ago2 was immunoprecipitated in cells that had been transfected with either *miR-145-5p* or *miR-145-3p* (Fig. 5A). Ago2 is an essential component of the RISC (16). Isolated Ago2-bound miRNAs were analyzed by RT-qPCR to confirm whether *miR-145-5p* and *miR-145-3p* bound to Ago2. In TE-8 cells, *miR-145-5p* transfectants demonstrated higher expression levels of *miR-145-5p* than mock transfectants, miR-control

Table III. Putative targets of *miR-145-3p* regulation in ESCC cells.

Entrez gene ID	Gene symbol	Gene name	TE-8 *miR-145-3p* transfectant	ESCC GSE20347 fold-change	Target site count	Prognosis P-value: TCGA OncoLnc data	
						ESCA	ESCC
10202	*DHRS2*	Dehydrogenase/reductase (SDR family) member 2	-2.69	2.02	1	0.047	0.708
1848	*DUSP6*	Dual specificity phosphatase 6	-2.61	1.00	1	0.456	0.469
55157	*DARS2*	Aspartyl-tRNA synthetase 2, mitochondrial	-2.09	1.17	2	0.504	0.706
6646	*SOAT1*	Sterol O-acyltransferase 1	-2.06	1.81	1	0.732	0.667
4430	*MYO1B*	Myosin IB	-1.98	1.61	2	0.372	0.856
2115	*ETV1*	Ets variant 1	-1.84	1.10	1	0.142	0.119
983	*CDK1*	Cyclin-dependent kinase 1	-1.63	1.95	1	0.621	0.136
1719	*DHFR*	Dihydrofolate reductase	-1.48	1.14	1	0.199	0.465
51053	*GMNN*	Geminin, DNA replication inhibitor	-1.46	1.37	1	0.274	0.189
23321	*TRIM2*	Tripartite motif containing 2	-1.35	1.45	1	<0.001[a]	0.037[a]
55697	*VAC14*	Vac14 homolog (S. cerevisiae)	-1.34	1.53	1	0.052	0.095
79789	*CLMN*	Calmin (calponin-like, transmembrane)	-1.33	1.79	2	0.519	0.352
5654	*HTRA1*	HtrA serine peptidase 1	-1.30	1.44	1	0.863	0.252
54830	*NUP62CL*	Nucleoporin 62 kDa C-terminal like	-1.28	1.10	1	0.313	0.313
204	*AK2*	Adenylate kinase 2	-1.24	1.21	2	0.691	0.972
126321	*MFSD12*	Major facilitator superfamily domain containing 12	-1.23	1.05	1	0.838	0.098
9532	*BAG2*	BCL2-associated athanogene 2	-1.20	1.80	2	0.109	0.563
51029	*DESI2*	Desumoylating isopeptidase 2	-1.18	1.25	2	0.261	0.19
6711	*SPTBN1*	Spectrin, β, non-erythrocytic 1	-1.18	1.21	1	0.515	0.504
1163	*CKS1B*	CDC28 protein kinase regulatory subunit 1B	-1.14	2.02	1	0.658	0.658
8534	*CHST1*	Carbohydrate (keratan sulfate Gal-6) Sulfotransferase 1	-1.14	1.52	1	0.943	0.983
5174	*PDZK1*	PDZ domain containing 1	-1.14	1.65	1	0.565	0.462
875	*CBS*	Cystathionine-β-synthase	-1.14	3.55	2	0.199	0.160
23516	*SLC39A14*	Solute carrier family 39 (zinc transporter), member 14	-1.12	2.68	1	0.322	0.101
6790	*AURKA*	Aurora kinase A	-1.07	2.17	1	0.322	0.051
79718	*TBL1XR1*	Transducin (β)-like 1 X-linked receptor 1	-1.06	1.30	1	0.579	0.377
23141	*ANKLE2*	Ankyrin repeat and LEM domain containing 2	-1.05	1.16	1	0.418	0.585
23649	*POLA2*	Polymerase (DNA directed), α 2, accessory subunit	-1.04	1.35	1	0.642	0.842
64151	*NCAPG*	Non-SMC condensin I complex, subunit G	-1.03	1.22	1	0.198	0.056
22848	*AAK1*	AP2 associated kinase 1	-1.03	1.27	3	0.634	0.346

[a]Poor prognosis with low expression. miR, microRNA; ESCC, esophageal squamous cell carcinoma; ESCA, esophageal carcinoma.

or *miR-145-3p* transfectants. Similarly, following *miR-145-3p* transfection, *miR-145-3p* was detected by Ago2 immunoprecipitation (Fig. 5B). *miR-145-5p* and *miR-145-3*p were demonstrated to bind to Ago2 separately and were incorporated into RISC, thereby demonstrating miRNA function.

Effects of co-transfection of mimic and inhibitor miR-145-3p into ESCC cells. To confirm the antitumor effects of *miR-145-3p*, rescue experiments were performed using mimic and inhibitor *miR-145-3p* with TE-8 cells (Fig. 6A). The rescue experiments indicated that cancer cell proliferation, migration and invasion

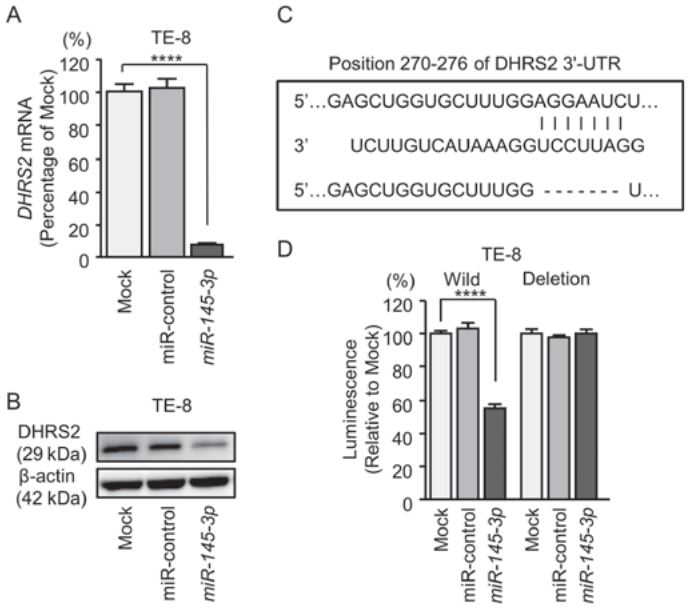

Figure 7. Direct regulation of *DHRS2* by *miR-145-3p* in esophageal squamous cell carcinoma cells. (A) Expression levels of *DHRS2* mRNA 72 h following transfection with 10 nM *miR-145-3p* into cell lines. Glucuronidase β was used as an internal control. (B) Expression of *DHRS2* proteins 72 h following transfection with *miR-145-3p*. β-actin was the loading control. (C) *miR-145-3p* binding site (positions 270-276) in the 3'-UTR of *DHRS2* mRNA. (D) Dual luciferase reporter assays using vectors encoding putative *miR-145-3p* target site in the *DHRS2* 3'-UTRs for wild-type and deleted regions. Renilla luciferase values were normalized to firefly luciferase values. ****P<0.0001. DHRS2, dehydrogenase/reductase member 2; miR, microRNA; UTR, untranslated region.

were rescued in *miR-145-3p* inhibitor transfectants compared with restored *miR-145-3p* mimic only (Fig. 6B-D).

Searching for putative targets regulated by miR-145-3p in ESCC cells. The strategy to identify *miR-145-3p* target genes is presented in Fig. 1. Gene expression analyses demonstrated that 1,374 genes were downregulated ($\log_2$ ratio <-1.0) in *miR-145-3p* transfected TE-8 cells compared with control transfectants. The present expression data were deposited in the GEO repository under accession no. GSE107008. Among these downregulated genes, genes that had putative *miR-145-3p* binding sites in their 3'-UTRs were selected using information in the TargetScan database. A total of 280 genes were identified. Then, 30 genes were selected by restricting the identified genes to those strongly upregulated in ESCC clinical specimens ($\log_2$ ratio >1.0; GEO accession no. GSE20347; Table III).

In this fashion, *DHRS2* was focused on, as its expression was the most downregulated in *miR-145-3p* transfectants and the most upregulated in ESCC clinical specimens. Additionally, *MYO1B* was examined, as it was more highly downregulated in *miR-145-3p* transfectants and was more upregulated in ESCC clinical specimens. In addition, our previous study had demonstrated that the activation of *MYO1B* was associated with cancer cell aggressiveness (20).

Direct regulation of DHRS2 and MYO1B by miR-145-3p in ESCC cells. The finding that *DHRS2* and *MYO1B* were downregulated by expression of *miR-145-3p* was further investigated (Figs. 7 and 8). ESCC cells (TE-8) that had been transfected with *miR-145-3p* were examined. Using RT-qPCR, it was demonstrated that *DHRS2* and *MYO1B* mRNA levels were significantly reduced by *miR-145-3p* transfection (Figs. 7A and 8A). Furthermore, western blot analysis was performed to measure the expression levels of DHRS2 and MYO1B proteins in the transfectants. Results demonstrated that the proteins were also reduced by *miR-145-3p* transfection (Figs. 7B and 8B).

Whether *miR-145-3p* directly regulated *DHRS2* and *MYO1B* genes in a sequence-dependent manner was then evaluated.

The Human TargetScan database predicted that *DHRS2* had 1 binding site (positions 270-276) for *miR-145-3p* in the 3'-UTR (Fig. 7C). Accordingly, luciferase reporter assays were carried out with vectors that included either the wild-type or deletion-type 3'-UTR of *DHRS2*. Co-transfection with *miR-145-3p* and vectors including the wild-type sequence significantly reduced luciferase activity compared with those in mock and miR-control transfectants in position 270-276 of the *DHRS2* 3'-UTR (Fig. 7D).

MYO1B had 2 binding sites (positions 88-94 and 1,117-1,123) for *miR-145-3p* in the 3'-UTR (Fig. 8C). Luciferase activities were significantly reduced in position 1,117-1,123 of the *MYO1B* 3'-UTR (Fig. 8D).

Effects of silencing DHRS2 and MYO1B in ESCC cells. Subsequently, siRNAs were transfected into TE-8 cells to examine the function of *DHRS2* and *MYO1B* in ESCC cells (Figs. 9 and 10). The mRNA and protein expression levels of *DHRS2* and *MYO1B* were decreased by si-*DHRS2* and si-*MYO1B*, respectively (Figs. 9A and B, and 10A and B). Subsequently, the effects of *DHRS2* or *MYO1B* knockdown on ESCC cell proliferation, migration and invasion were investigated.

Cancer cell proliferation was significantly suppressed in si-*DHRS2* or si-*MYO1B* transfectants compared with mock and si-RNA-control transfectants. Additionally, migration and invasion activities were significantly inhibited in si-DHRS2

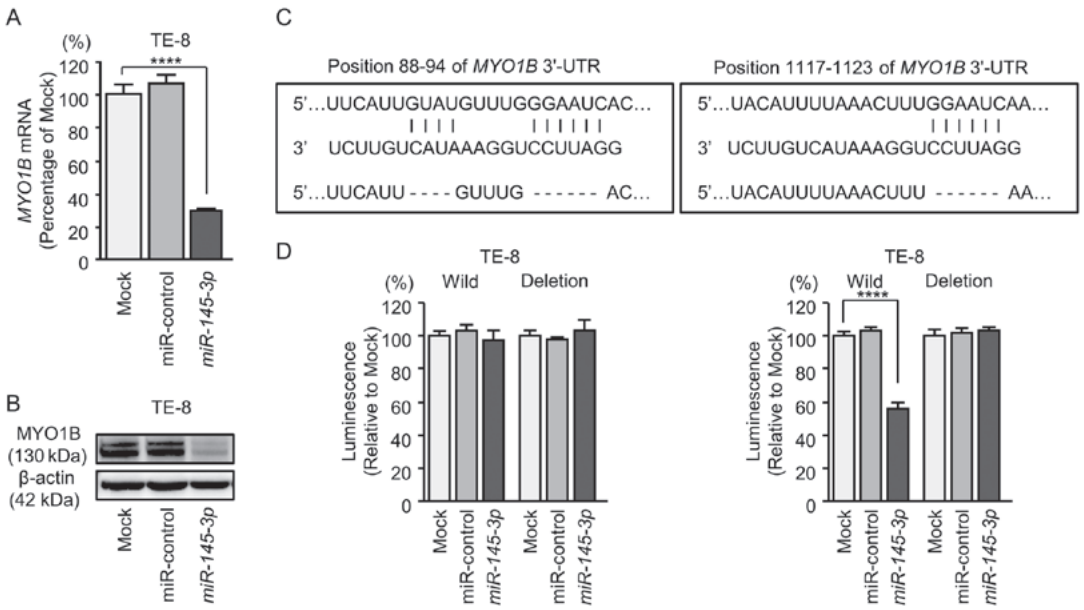

Figure 8. Direct regulation of *MYO1B* by *miR-145-3p* in esophageal squamous cell carcinoma cells. (A) Expression levels of *MYO1B* mRNA 72 h following transfection with 10 nM *miR-145-3p* into cell lines. Glucuronidase β was used as an internal control. (B) Expression of *MYO1B* proteins 72 h following transfection with *miR-145-3p*. β-actin was the loading control. (C) *miR-145-3p* binding sites (positions 88-94 or positions 1,117-1,123) in the 3'-UTR of *MYO1B* mRNA. (D) Dual luciferase reporter assays using vectors encoding putative *miR-145-3p* target sites in the *MYO1B* 3'-UTRs for both wild-type and deleted regions. Renilla luciferase values were normalized to firefly luciferase values. ****P<0.0001. MYO1B, myosin IB; miR, microRNA.

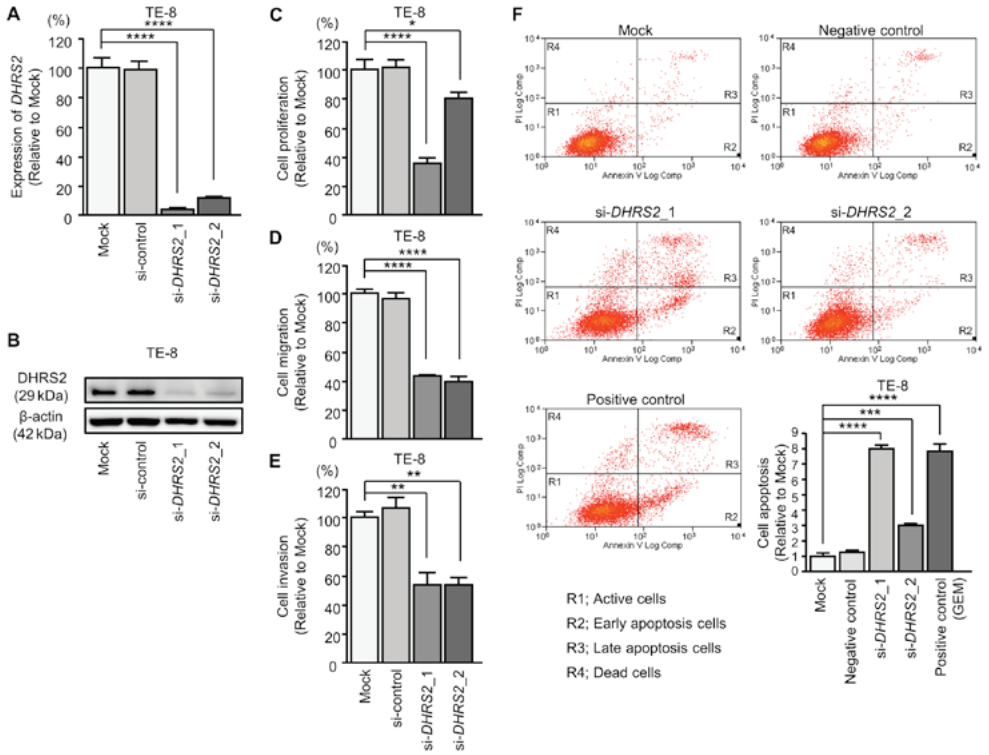

Figure 9. Effects of silencing *DHRS2* in ESCC cells. (A) *DHRS2* mRNA expression 72 h following transfection of 10 nM si-*DHRS2* into ESCC cell lines. Glucuronidase β was used as an internal control. (B) Protein expression 72 h following transfection with si-*DHRS2*. β-actin was the loading control. (C) Cell proliferation was determined with XTT assays 72 h following transfection with 10 nM si-*DHRS2*. (D) Results of cell migration assays. (E) Results of Matrigel invasion assays. (F) Results of cell apoptosis assays. *P<0.05, **P<0.01, ***P<0.001, ****P<0.0001. DHRS2, dehydrogenase/reductase member 2; ESCC, esophageal squamous cell carcinoma; si, small interfering RNA.

or si-MYO1B transfectants (Figs. 9C-E and 10C-E). In the apoptosis assays, si-*DHRS2*_1/si-*DHRS2*_2 and si-*MYO1B*_1/si-*MYO1B*_2 transfections significantly increased apoptotic TE-8 cells (Figs. 9F and 10F).

Expression of DHRS2 and MYO1B in ESCC clinical specimens. Based upon the findings above, it was of great interest to use RT-qPCR to determine the expression levels of *DHRS2* and *MYO1B* in clinical specimens. *DHRS2* and

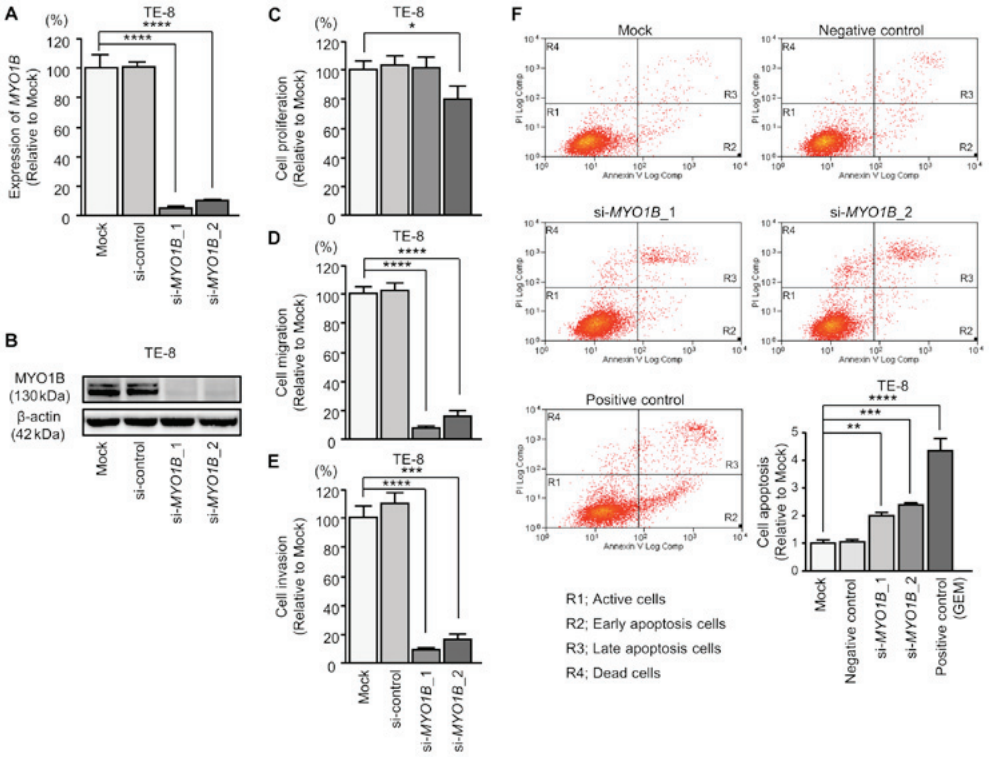

Figure 10. Effects of silencing *MYO1B* in ESCC cells. (A) *MYO1B* mRNA expression 72 h following transfection of 10 nM si-*MYO1B* into ESCC cell lines. Glucuronidase β was used as an internal control. (B) Protein expression 72 h following transfection with si-*MYO1B*. β-actin was the loading control. (C) Cell proliferation was determined with XTT assays 72 h following transfection with 10 nM si-*MYO1B*. (D) Results of cell migration assays. (E) Results of Matrigel invasion assays. (F) Results of cell apoptosis assays. *P<0.05, **P<0.01, ***P<0.001, ****P<0.0001. MYO1B, myosin IB; ESCC, esophageal squamous cell carcinoma; si, small interfering RNA.

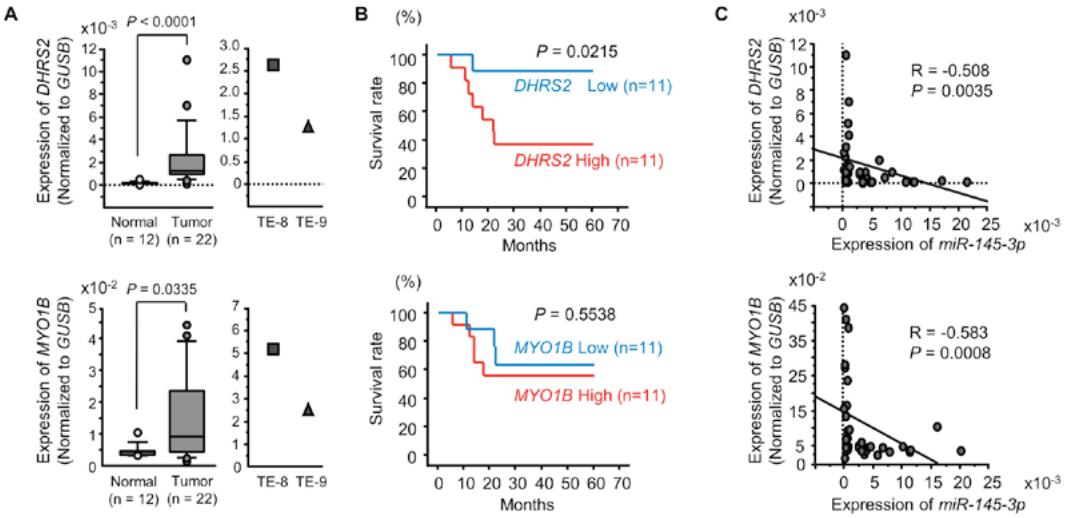

Figure 11. Expression of *DHRS2* and ^{MYO1B} in ESCC clinical specimens. (A) Expression levels of *DHRS2* and *MYO1B* in ESCC clinical specimens. *GUSB* was the internal control. (B) The 5-year survival rates were analyzed by Kaplan-Meier survival curves and log-rank statistics. (C) Spearman's rank test was used to evaluate the correlation between *DHRS2* or *MYO1B* expression and *miR-145-3p*. DHRS2, dehydrogenase/reductase member 2; MYO1B, myosin IB; ESCC, esophageal squamous cell carcinoma; miR, microRNA; GUSB, glucuronidase β.

MYO1B expression levels were significantly upregulated in ESCC tumor tissues (Fig. 11A). Additionally, the 5-year survival rates of ESSC patients were significantly shorter in those with elevated *DHRS2* expression compared with those with low expression (Fig. 11B). There was no significant association between the expression levels of *MYO1B* and the survival rate (Fig. 11B).

Spearman's rank test demonstrated a negative correlation between the expression of *DHRS2* and *miR-145-3p*, and *MYO1B* and *miR-145-3p* (Fig. 11C). Furthermore, the protein expression levels of DHRS2 and MYO1B were examined in ESCC clinical specimens by immunostaining. Both DHRS2 and MYO1B were strongly expressed in cancer tissues, but not in noncancerous epithelia (Fig. 12).

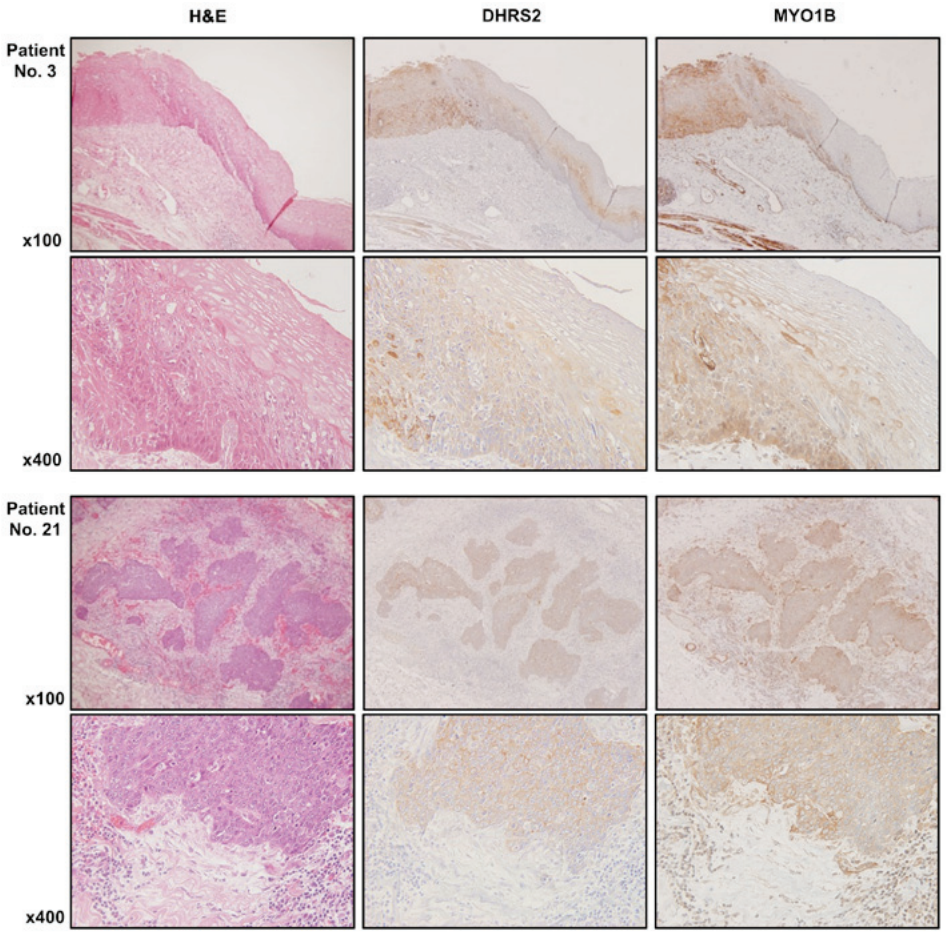

Figure 12. Immunohistochemical analysis of esophageal squamous cell carcinoma clinical samples. Immunostaining demonstrated that DHRS2 and MYO1B were strongly expressed in cancer tissues whereas strong expression was not observed in non-cancerous epithelia (x100 and x400 magnification fields). DHRS2, dehydrogenase/reductase member 2; MYO1B, myosin IB; H&E, hematoxylin and eosin.

Exploration of downstream targets regulated by si-DHRS2 and si-MYO1B in ESCC. The present strategy for selecting downstream genes regulated by *DHRS2* and *MYO1B* is demonstrated in Fig. 2. A total of 756 genes were commonly downregulated ($\log_2$ ratio <-1.5) in si-*DHRS2*-transfected TE-8 cells. The upregulated genes in ESCC tissues were also assessed by GEO database analyses (GEO accession no. GSE20347). With that approach, 85 candidate genes downstream from *DHRS2* were identified (Table IV). Furthermore, a total of 334 genes were commonly downregulated ($\log_2$ ratio <-1.5) in si-*MYO1B*-transfected TE-8 cells. In a similar approach, 32 candidate genes downstream from *MYO1B* were identified (Table V).

Discussion

Downregulation of *miR-145-5p* has frequently been observed in a wide range of cancers, including ESCC (32). A number of previous studies have demonstrated that ectopic expression of *miR-145-5p* suppressed cancer cell proliferation, migration, invasion and drug resistance both *in vitro* and *in vivo* (25,26,33). Notably, the promoter region of pre-*miR-145* has a p53 response element and its expression is controlled by activation of p53 under various conditions (34). Therefore, both strands of the *miR-145* duplex are pivotal tumor suppressor miRNAs controlled by p53.

Analyses of the miRNA expression signatures demonstrated that certain miRNA passenger strands were downregulated and acted as antitumor miRNAs in several cancers, e.g., *miR-145-3p*, *miR-150-3*p, *miR-148a-5p* and *miR-99a-3p* (20,24,35,36). Our previous studies demonstrated that antitumor *miR-145-3p* directly targeted oncogenes, e.g., *MTDH* in lung adenocarcinoma, *UHRF1* in bladder cancer, *MYO1B* in head and neck cancer and *MELK*, *NCAPG*, *BUB1* and *CDK1* in prostate cancer (17-20). Another group demonstrated that *miR-145-3p* inhibited cell growth, motility and chemotaxis in non-small cell lung cancer by targeting pyruvate dehydrogenase kinase 1 through suppressing the mechanistic target of rapamycin pathway (37). These findings indicated that antitumor miR-145-3p is associated with cancer pathogenesis.

Exploring the RNA network controlled by antitumor *miR-145-3p* expands the understanding of the novel molecular pathogenesis of ESCC. In the present study, 30 genes were identified as putative oncogenes based on *miR-145-3p* regulation in ESCC cells. Among these genes, the following 3 were reported to be cancer-promoting genes in ESCC: cyclin dependent kinase 1 (*CDK1*), aurora kinase A (*AURKA*) and transducin β like 1 X-linked receptor 1 (*TBL1XR1*) (38-43). Identification of the target genes controlled by *miR-145-3p* is important for understanding the underlying molecular pathogenesis of ESCC.

Table IV. Putative targets of si-*DHRS2* regulation in ESCC cells.

Entrez gene ID	Gene symbol	Gene name	ESCC GSE20347 fold-change	TE-8 si-*DHRS2* transfectant
1592	*CYP26A1*	Cytochrome P450, family 26, subfamily A, polypeptide 1	1.86	-3.78
10112	*KIF20A*	Kinesin family member 20A	1.50	-3.28
259266	*ASPM*	Asp (abnormal spindle) homolog, microcephaly associated (*Drosophila*)	1.56	-3.08
27074	*LAMP3*	Lysosomal-associated membrane protein 3	1.56	-3.03
11098	*PRSS23*	Protease, serine, 23	1.86	-3.02
10202	*DHRS2*	Dehydrogenase/reductase (SDR family) member 2	2.02	-2.98
4322	*MMP13*	Matrix metallopeptidase 13 (collagenase 3)	5.12	-2.93
79075	*DSCC1*	DNA replication and sister chromatid cohesion 1	1.95	-2.80
983	*CDK1*	Cyclin-dependent kinase 1	1.95	-2.79
332	*BIRC5*	Baculoviral IAP repeat containing 5	1.59	-2.72
995	*CDC25C*	Cell division cycle 25C	1.51	-2.71
11065	*UBE2C*	Ubiquitin-conjugating enzyme E2C	1.68	-2.70
4751	*NEK2*	NIMA-related kinase 2	1.66	-2.70
1033	*CDKN3*	Cyclin-dependent kinase inhibitor 3	1.94	-2.70
11339	*OIP5*	Opa interacting protein 5	1.63	-2.68
2842	*GPR19*	G protein-coupled receptor 19	2.12	-2.64
10615	*SPAG5*	Sperm associated antigen 5	1.59	-2.60
9055	*PRC1*	Protein regulator of cytokinesis 1	1.58	-2.60
699	*BUB1*	BUB1 mitotic checkpoint serine/threonine kinase	2.04	-2.59
991	*CDC20*	Cell division cycle 20	1.54	-2.58
55355	*HJURP*	Holliday junction recognition protein	1.79	-2.51
7153	*TOP2A*	Topoisomerase (DNA) II alpha 170 kDa	1.91	-2.46
10403	*NDC80*	NDC80 kinetochore complex component	1.76	-2.45
55388	*MCM10*	Minichromosome maintenance complex component 10	1.90	-2.45
2263	*FGFR2*	Fibroblast growth factor receptor 2	1.65	-2.44
3161	*HMMR*	Hyaluronan-mediated motility receptor (RHAMM)	1.60	-2.42
1063	*CENPF*	Centromere protein F, 350/400 kDa	2.31	-2.40
7272	*TTK*	TTK protein kinase	1.58	-2.36
9401	*RECQL4*	RecQ protein-like 4	1.92	-2.35
9355	*LHX2*	LIM homeobox 2	2.63	-2.33
22836	*RHOBTB3*	Rho-related BTB domain containing 3	1.98	-2.33
54478	*FAM64A*	Family with sequence similarity 64, member A	1.60	-2.33
9133	*CCNB2*	Cyclin B2	1.68	-2.27
9787	*DLGAP5*	Discs, large (*Drosophila*) homolog-associated protein 5	1.72	-2.26
9156	*EXO1*	Exonuclease 1	1.89	-2.26
3833	*KIFC1*	Kinesin family member C1	2.15	-2.19
347733	*TUBB2B*	Tubulin, beta 2B class IIb	1.86	-2.18
220134	*SKA1*	Spindle and kinetochore associated complex subunit 1	1.73	-2.18
4291	*MLF1*	Myeloid leukemia factor 1	1.90	-2.15
8438	*RAD54L*	RAD54-like (S. cerevisiae)	2.31	-2.14
79019	*CENPM*	Centromere protein M	2.10	-2.14
51514	*DTL*	Denticleless E3 ubiquitin protein ligase homolog (*Drosophila*)	1.62	-2.12
55872	*PBK*	PDZ binding kinase	1.70	-2.11
3790	*KCNS3*	Potassium voltage-gated channel, modifier subfamily S, member 3	2.32	-2.11
51512	*GTSE1*	G-2 and S-phase expressed 1	2.02	-2.10
9493	*KIF23*	Kinesin family member 23	1.96	-2.10
5983	*RFC3*	Replication factor C (activator 1) 3, 38 kDa	1.74	-2.09
81611	*ANP32E*	Acidic (leucine-rich) nuclear phosphoprotein 32 family, member E	1.52	-2.07

Table IV. Continued.

Entrez gene ID	Gene symbol	Gene name	ESCC GSE20347 fold-change	TE-8 si-*DHRS2* transfectant
83461	*CDCA3*	Cell division cycle associated 3	2.14	-2.05
23350	*U2SURP*	U2 snRNP-associated SURP domain containing	1.62	-2.01
6790	*AURKA*	Aurora kinase A	2.17	-2.00
55165	*CEP55*	Centrosomal protein 55 kDa	1.94	-1.99
80178	*C16orf59*	Chromosome 16 open reading frame 59	1.61	-1.98
2305	*FOXM1*	Forkhead box M1	2.16	-1.96
24137	*KIF4A*	Kinesin family member 4A	1.95	-1.94
22974	*TPX2*	TPX2, microtubule-associated	1.65	-1.94
55215	*FANCI*	Fanconi anemia, complementation group I	1.70	-1.91
10635	*RAD51AP1*	RAD51 associated protein 1	2.20	-1.88
993	*CDC25A*	Cell division cycle 25A	1.88	-1.88
2175	*FANCA*	Fanconi anemia, complementation group A	1.93	-1.85
4171	*MCM2*	Minichromosome maintenance complex component 2	2.55	-1.82
2491	*CENPI*	Centromere protein I	1.81	-1.81
655	*BMP7*	Bone morphogenetic protein 7	1.54	-1.77
4998	*ORC1*	Origin recognition complex, subunit 1	1.53	-1.76
10036	*CHAF1A*	Chromatin assembly factor 1, subunit A (p150)	1.75	-1.76
4085	*MAD2L1*	MAD2 mitotic arrest deficient-like 1 (yeast)	1.67	-1.76
3149	*HMGB3*	High mobility group box 3	2.01	-1.74
29028	*ATAD2*	ATPase family, AAA domain containing 2	1.96	-1.73
9837	*GINS1*	GINS complex subunit 1 (Psf1 homolog)	1.64	-1.73
51659	*GINS2*	GINS complex subunit 2 (Psf2 homolog)	1.86	-1.72
5984	*RFC4*	Replication factor C (activator 1) 4, 37 kDa	2.08	-1.69
55839	*CENPN*	Centromere protein N	1.72	-1.66
7078	*TIMP3*	TIMP metallopeptidase inhibitor 3	2.23	-1.66
27346	*TMEM97*	Transmembrane protein 97	1.67	-1.65
9928	*KIF14*	Kinesin family member 14	2.14	-1.64
3625	*INHBB*	Inhibin, β B	1.75	-1.63
10721	*POLQ*	Polymerase (DNA directed), θ	1.51	-1.62
1663	*DDX11*	DEAD/H (Asp-Glu-Ala-Asp/His) box helicase 11	2.08	-1.60
9319	*TRIP13*	Thyroid hormone receptor interactor 13	2.02	-1.58
4605	*MYBL2*	V-myb avian myeloblastosis viral oncogene homolog-like 2	3.08	-1.56
51762	*RAB8B*	RAB8B, member RAS oncogene family	1.76	-1.54
91860	*CALML4*	Calmodulin-like 4	1.90	-1.54
10293	*TRAIP*	TRAF interacting protein	1.50	-1.52
2237	*FEN1*	Flap structure-specific endonuclease 1	1.54	-1.51
55753	*OGDHL*	Oxoglutarate dehydrogenase-like	2.37	-1.51

DHRS2, dehydrogenase/reductase member 2; ESCC, esophageal squamous cell carcinoma; si, small interfering RNA.

The present study demonstrated that both *DHRS2* and *MYO1B* were directly regulated by *miR-145-3p* in ESCC cells. Overexpression of *DHRS2* and *MYO1B* was observed in ESCC clinical specimens, and overexpression was associated with cancer cell aggressiveness. *DHRS2* was initially cloned from a HepG2 human hepatocarcinoma cDNA library and named *HEP27* (44). *DHRS2* is a member of the short-chain dehydrogenase/reductase (SDR) family that metabolizes many different compounds (45). HEP27 protein interacts with *MDM2*, which is a negative regulator of p53, resulting in p53 stabilization and induction of p53 transcriptional target genes (46). More recently, downregulation of *DHRS2* was reported in ESCC tissues and its downregulation was associated with ESCC aggressiveness and clinical staging (47). Thus, that report arrived at the opposite conclusions from those in our study. Further investigation of *DHRS2* function in cancer cells will be necessary.

MYO1B is a member of the membrane-associated class I myosin family and it bridges membrane and actin cytoskeleton

Table V. Putative targets of si-*MYO1B* regulation in ESCC cells.

Entrez gene ID	Gene symbol	Gene name	ESCC GSE20347 fold-change	TE-8 si-*MYO1B* transfectant
4430	*MYO1B*	Myosin IB	1.61	-3.60
347733	*TUBB2B*	Tubulin, β 2B class IIb	1.86	-2.89
9837	*GINS1*	GINS complex subunit 1 (Psf1 homolog)	1.64	-2.72
4322	*MMP13*	Matrix metallopeptidase 13 (collagenase 3)	5.12	-2.66
79075	*DSCC1*	DNA replication and sister chromatid cohesion 1	1.95	-2.55
4312	*MMP1*	Matrix metallopeptidase 1 (interstitial collagenase)	6.54	-2.40
51514	*DTL*	Denticleless E3 ubiquitin protein ligase homolog (*Drosophila*)	1.62	-2.38
4319	*MMP10*	Matrix metallopeptidase 10 (stromelysin 2)	4.51	-2.28
23657	*SLC7A11*	Solute carrier family 7 (anionic amino acid transporter light chain, xc- system), member 11	1.97	-2.20
5983	*RFC3*	Replication factor C (activator 1) 3, 38 kDa	1.74	-2.11
10202	*DHRS2*	Dehydrogenase/reductase (SDR family) member 2	2.02	-2.04
2491	*CENPI*	Centromere protein I	1.81	-2.01
4085	*MAD2L1*	MAD2 mitotic arrest deficient-like 1 (yeast)	1.67	-1.99
6574	*SLC20A1*	Solute carrier family 20 (phosphate transporter), member 1	1.52	-1.91
4998	*ORC1*	Origin recognition complex, subunit 1	1.53	-1.84
81611	*ANP32E*	Acidic (leucine-rich) nuclear phosphoprotein 32 family, member E	1.52	-1.83
10669	*CGREF1*	Cell growth regulator with EF-hand domain 1	1.62	-1.81
55388	*MCM10*	Minichromosome maintenance complex component 10	1.90	-1.79
2119	*ETV5*	Ets variant 5	2.05	-1.79
11199	*ANXA10*	Annexin A10	2.06	-1.76
655	*BMP7*	Bone morphogenetic protein 7	1.54	-1.73
983	*CDK1*	Cyclin-dependent kinase 1	1.95	-1.72
55872	*PBK*	PDZ binding kinase	1.70	-1.70
4072	*EPCAM*	Epithelial cell adhesion molecule	2.56	-1.68
8914	*TIMELESS*	Timeless circadian clock	1.54	-1.65
9518	*GDF15*	Growth differentiation factor 15	1.58	-1.65
55215	*FANCI*	Fanconi anemia, complementation group I	1.70	-1.62
11339	*OIP5*	Opa interacting protein 5	1.63	-1.61
10635	*RAD51AP1*	RAD51 associated protein 1	2.20	-1.59
332	*BIRC5*	Baculoviral IAP repeat containing 5	1.59	-1.58
995	*CDC25C*	Cell division cycle 25C	1.51	-1.54
8438	*RAD54L*	RAD54-like (S. cerevisiae)	2.31	-1.52

MYO1B, myosin IB; ESCC, esophageal squamous cell carcinoma; si, small interfering RNA.

in several cellular processes (48). It was recently demonstrated that overexpression of *MYO1B* is associated with head and neck cancer pathogenesis (20). Importantly, antitumor *miR-145-3p* directly regulated expression of *MYO1B* in head and neck cells (20). A previous *in vivo* study demonstrated that downregulation of *MYO1B* inhibited cervical lymph node metastasis in head and neck cancer cells (49). These findings indicate that aberrantly expressed *MYO1B* is associated with cancer cell aggressiveness and metastasis. *MYO1B* may be a novel diagnostic and therapeutic target for patients with ESCC.

Downstream genes modulated by *DHRS2* or *MYO1B* in ESCC cells were investigated. Previous studies have demonstrated that several aberrantly expressed oncogenes (*CDK1*, *BIRC5*, *BUB1*, *TOP2A*, *CENPF*, *FOXM1* and *AURKA*) enhanced cancer cell aggressiveness (38,50-54). Notably, *MMP13* may be controlled by *DHRS2* and *MYO1B* in ESCC cells. Our recent study demonstrated that overexpression of *MMP13* occurred in ESCC clinical specimens and the expression of *MMP13* promoted cancer cell proliferation, migration and invasion (28). Identification of the downstream genes regulated by the *miR-145-3p*/*DHRS2* or *miR-145-3p*/*MYO1B* axis may improve the understanding of ESCC aggressiveness.

In conclusion, genes controlled by the antitumor activity of *miR-145-3p* were closely associated with ESCC pathogenesis. Association of the passenger strand of miRNA is a novel concept of cancer research. *DHRS2* and *MYO1B* were directly

regulated by *miR-145-3p* in ESCC cells. Aberrantly expressed *DHRS2* and *MYO1B* enhanced ESCC cell aggressiveness. Elucidation of antitumor miRNAs controlling RNA networks may provide novel prognostic markers and therapeutic targets for this disease.

Acknowledgements

Not applicable.

Funding

The present study was supported by KAKENHI grants nos. 15K10801, 18K16322, 16K10508, 17K10706, 16K10510, 18K08687, 18K08626 and 17H04285.

Availability of data and materials

All data generated or analyzed during this study are included in this published article.

Authors' contributions

MS and TI performed the majority of the study and wrote the manuscript. NS and SN designed the study and wrote the manuscript. YY, TAra, YK and HK performed the experiments and data interpretation. TAri, KS, IO, YU and KM provided sample collection and clinical support. All authors reviewed, edited and approved the final version of the manuscript.

Ethics approval and consent to participate

The present study was approved by the Bioethics Committee of Kagoshima University (Kagoshima, Japan; approval no. 28-65). Written prior informed consent and approval were obtained from all patients.

Patient consent for publication

All patients had provided written informed consent prior to surgery.

Competing interests

The authors declare that they have no competing interests.

References

1. Ferlay J, Soerjomataram I, Dikshit R, Eser S, Mathers C, Rebelo M, Parkin DM, Forman D and Bray F: Cancer incidence and mortality worldwide: Sources, methods and major patterns in GLOBOCAN 2012. Int J Cancer 136: E359-E386, 2015.
2. Enzinger PC and Mayer RJ: Esophageal cancer. N Engl J Med 349: 2241-2252, 2003.
3. Pennathur A, Gibson MK, Jobe BA and Luketich JD: Oesophageal carcinoma. Lancet 381: 400-412, 2013.
4. Mariette C, Piessen G and Triboulet JP: Therapeutic strategies in oesophageal carcinoma: Role of surgery and other modalities. Lancet Oncol 8: 545-553, 2007.
5. Cai XW, Yu WW, Yu W, Zhang Q, Feng W, Liu MN, Sun MH, Xiang JQ, Zhang YW and Fu XL: Tissue-based quantitative proteomics to screen and identify the potential biomarkers for early recurrence/metastasis of esophageal squamous cell carcinoma. Cancer Med 7: 2504-2517, 2018.
6. Cooper JS, Guo MD, Herskovic A, Macdonald JS, Martenson JA Jr, Al-Sarraf M, Byhardt R, Russell AH, Beitler JJ, Spencer S, *et al*; Radiation Therapy Oncology Group: Chemoradiotherapy of locally advanced esophageal cancer: Long-term follow-up of a prospective randomized trial (RTOG 85-01). JAMA 281: 1623-1627, 1999.
7. Natsugoe S, Ikeda M, Baba M, Churei H, Hiraki Y, Nakajo M and Aikou T; Kyushu Study Group for Adjuvant Therapy of Esophageal Cancer: Long-term survivors of advanced esophageal cancer without surgical treatment: A multicenter questionnaire survey in Kyushu, Japan. Dis Esophagus 16: 239-242, 2003.
8. Ando N, Kato H, Igaki H, Shinoda M, Ozawa S, Shimizu H, Nakamura T, Yabusaki H, Aoyama N, Kurita A, *et al*: A randomized trial comparing postoperative adjuvant chemotherapy with cisplatin and 5-fluorouracil versus preoperative chemotherapy for localized advanced squamous cell carcinoma of the thoracic esophagus (JCOG9907). Ann Surg Oncol 19: 68-74, 2012.
9. Dutton SJ, Ferry DR, Blazeby JM, Abbas H, Dahle-Smith A, Mansoor W, Thompson J, Harrison M, Chatterjee A, Falk S, *et al*: Gefitinib for oesophageal cancer progressing after chemotherapy (COG): A phase 3, multicentre, double-blind, placebo-controlled randomised trial. Lancet Oncol 15: 894-904, 2014.
10. Suntharalingam M, Winter K, Ilson D, Dicker AP, Kachnic L, Konski A, Chakravarthy AB, Anker CJ, Thakrar H, Horiba N, *et al*: Effect of the addition of cetuximab to paclitaxel, cisplatin, and radiation therapy for patients with esophageal cancer: The NRG Oncology RTOG 0436 phase 3 randomized clinical trial. JAMA Oncol 3: 1520-1528, 2017.
11. Hemmatzadeh M, Mohammadi H, Karimi M, Musavishenas MH and Baradaran B: Differential role of microRNAs in the pathogenesis and treatment of Esophageal cancer. Biomed Pharmacother 82: 509-519, 2016.
12. Lin DC, Wang MR and Koeffler HP: Genomic and epigenomic aberrations in esophageal squamous cell carcinoma and implications for patients. Gastroenterology 154: 374-389, 2018.
13. Bartel DP: MicroRNAs: Genomics, biogenesis, mechanism, and function. Cell 116: 281-297, 2004.
14. Chen CZ: MicroRNAs as oncogenes and tumor suppressors. N Engl J Med 353: 1768-1771, 2005.
15. Friedman RC, Farh KK, Burge CB and Bartel DP: Most mammalian mRNAs are conserved targets of microRNAs. Genome Res 19: 92-105, 2009.
16. Bartel DP: MicroRNAs: Target recognition and regulatory functions. Cell 136: 215-233, 2009.
17. Mataki H, Seki N, Mizuno K, Nohata N, Kamikawaji K, Kumamoto T, Koshizuka K, Goto Y and Inoue H: Dual-strand tumor-suppressor microRNA-145 (miR-145-5p and miR-145-3p) coordinately targeted MTDH in lung squamous cell carcinoma. Oncotarget 7: 72084-72098, 2016.
18. Matsushita R, Yoshino H, Enokida H, Goto Y, Miyamoto K, Yonemori M, Inoguchi S, Nakagawa M and Seki N: Regulation of UHRF1 by dual-strand tumor-suppressor microRNA-145 (miR-145-5p and miR-145-3p): Inhibition of bladder cancer cell aggressiveness. Oncotarget 7: 28460-28487, 2016.
19. Goto Y, Kurozumi A, Arai T, Nohata N, Kojima S, Okato A, Kato M, Yamazaki K, Ishida Y, Naya Y, *et al*: Impact of novel miR-145-3p regulatory networks on survival in patients with castration-resistant prostate cancer. Br J Cancer 117: 409-420, 2017.
20. Yamada Y, Koshizuka K, Hanazawa T, Kikkawa N, Okato A, Idichi T, Arai T, Sugawara S, Katada K, Okamoto Y, *et al*: Passenger strand of miR-145-3p acts as a tumor-suppressor by targeting MYO1B in head and neck squamous cell carcinoma. Int J Oncol 52: 166-178, 2018.
21. Schwarz DS, Hutvágner G, Du T, Xu Z, Aronin N and Zamore PD: Asymmetry in the assembly of the RNAi enzyme complex. Cell 115: 199-208, 2003.
22. Mah SM, Buske C, Humphries RK and Kuchenbauer F: miRNA*: A passenger stranded in RNA-induced silencing complex? Crit Rev Eukaryot Gene Expr 20: 141-148, 2010.
23. Liu WW, Meng J, Cui J and Luan YS: Characterization and Function of MicroRNA*s in Plants. Front Plant Sci 8: 2200, 2017.
24. Osako Y, Seki N, Koshizuka K, Okato A, Idichi T, Arai T, Omoto I, Sasaki K, Uchikado Y, Kita Y, *et al*: Regulation of SPOCK1 by dual strands of pre-miR-150 inhibit cancer cell migration and invasion in esophageal squamous cell carcinoma. J Hum Genet 62: 935-944, 2017.
25. Sachdeva M and Mo YY: MicroRNA-145 suppresses cell invasion and metastasis by directly targeting mucin 1. Cancer Res 70: 378-387, 2010.

26. Kano M, Seki N, Kikkawa N, Fujimura L, Hoshino I, Akutsu Y, Chiyomaru T, Enokida H, Nakagawa M and Matsubara H: miR-145, miR-133a and miR-133b: Tumor-suppressive miRNAs target FSCN1 in esophageal squamous cell carcinoma. Int J Cancer 127: 2804-2814, 2010.
27. Nishihira T, Hashimoto Y, Katayama M, Mori S and Kuroki T: Molecular and cellular features of esophageal cancer cells. J Cancer Res Clin Oncol 119: 441-449, 1993.
28. Osako Y, Seki N, Kita Y, Yonemori K, Koshizuka K, Kurozumi A, Omoto I, Sasaki K, Uchikado Y, Kurahara H, *et al*: Regulation of MMP13 by antitumor microRNA-375 markedly inhibits cancer cell migration and invasion in esophageal squamous cell carcinoma. Int J Oncol 49: 2255-2264, 2016.
29. Yonemori K, Seki N, Kurahara H, Osako Y, Idichi T, Arai T, Koshizuka K, Kita Y, Maemura K and Natsugoe S: ZFP36L2 promotes cancer cell aggressiveness and is regulated by antitumor microRNA-375 in pancreatic ductal adenocarcinoma. Cancer Sci 108: 124-135, 2017.
30. Yoshino H, Chiyomaru T, Enokida H, Kawakami K, Tatarano S, Nishiyama K, Nohata N, Seki N and Nakagawa M: The tumour-suppressive function of miR-1 and miR-133a targeting TAGLN2 in bladder cancer. Br J Cancer 104: 808-818, 2011.
31. Harada K, Baba Y, Ishimoto T, Kosumi K, Tokunaga R, Izumi D, Ohuchi M, Nakamura K, Kiyozumi Y, Kurashige J, *et al*: Suppressor microRNA-145 is epigenetically regulated by promoter hypermethylation in esophageal squamous cell carcinoma. Anticancer Res 35: 4617-4624, 2015.
32. Kita Y, Nishizono Y, Okumura H, Uchikado Y, Sasaki K, Matsumoto M, Setoyama T, Tanoue K, Omoto I, Mori S, *et al*: Clinical and biological impact of cyclin-dependent kinase subunit 2 in esophageal squamous cell carcinoma. Oncol Rep 31: 1986-1992, 2014.
33. Zeng JF, Ma XQ, Wang LP and Wang W: MicroRNA-145 exerts tumor-suppressive and chemo-resistance lowering effects by targeting CD44 in gastric cancer. World J Gastroenterol 23: 2337-2345, 2017.
34. Sachdeva M, Zhu S, Wu F, Wu H, Walia V, Kumar S, Elble R, Watabe K and Mo YY: p53 represses c-Myc through induction of the tumor suppressor miR-145. Proc Natl Acad Sci USA 106: 3207-3212, 2009.
35. Arai T, Okato A, Yamada Y, Sugawara S, Kurozumi A, Kojima S, Yamazaki K, Naya Y, Ichikawa T and Seki N: Regulation of NCAPG by miR-99a-3p (passenger strand) inhibits cancer cell aggressiveness and is involved in CRPC. Cancer Med 7: 1988-2002, 2018.
36. Idichi T, Seki N, Kurahara H, Fukuhisa H, Toda H, Shimonosono M, Okato A, Arai T, Kita Y, Mataki Y, *et al*: Molecular pathogenesis of pancreatic ductal adenocarcinoma: Impact of passenger strand of pre-miR-148a on gene regulation. Cancer Sci 109: 2013-2026, 2018.
37. Chen GM, Zheng AJ, Cai J, Han P, Ji HB and Wang LL: microRNA-145-3p inhibits non-small cell lung cancer cell migration and invasion by targeting PDK1 via the mTOR signaling pathway. J Cell Biochem 119: 885-895, 2018.
38. Dutertre S, Descamps S and Prigent C: On the role of aurora-A in centrosome function. Oncogene 21: 6175-6183, 2002.
39. Fung TK, Yam CH and Poon RY: The N-terminal regulatory domain of cyclin A contains redundant ubiquitination targeting sequences and acceptor sites. Cell Cycle 4: 1411-1420, 2005.
40. Li JY, Daniels G, Wang J and Zhang X: TBL1XR1 in physiological and pathological states. Am J Clin Exp Urol 3: 13-23, 2015.
41. Liu L, Lin C, Liang W, Wu S, Liu A, Wu J, Zhang X, Ren P, Li M and Song L: TBL1XR1 promotes lymphangiogenesis and lymphatic metastasis in esophageal squamous cell carcinoma. Gut 64: 26-36, 2015.
42. Tamotsu K, Okumura H, Uchikado Y, Kita Y, Sasaki K, Omoto I, Owaki T, Arigami T, Uenosono Y, Nakajo A, *et al*: Correlation of Aurora-A expression with the effect of chemoradiation therapy on esophageal squamous cell carcinoma. BMC Cancer 15: 323, 2015.
43. Zhang HF, Alshareef A, Wu C, Jiao JW, Sorensen PH, Lai R, Xu LY and Li EM: miR-200b induces cell cycle arrest and represses cell growth in esophageal squamous cell carcinoma. Carcinogenesis 37: 858-869, 2016.
44. Gabrielli F, Donadel G, Bensi G, Heguy A and Melli M: A nuclear protein, synthesized in growth-arrested human hepatoblastoma cells, is a novel member of the short-chain alcohol dehydrogenase family. Eur J Biochem 232: 473-477, 1995.
45. Gabrielli F and Tofanelli S: Molecular and functional evolution of human DHRS2 and DHRS4 duplicated genes. Gene 511: 461-469, 2012.
46. Deisenroth C, Thorner AR, Enomoto T, Perou CM and Zhang Y: Mitochondrial Hep27 is a c-Myb target gene that inhibits Mdm2 and stabilizes p53. Mol Cell Biol 30: 3981-3993, 2010.
47. Zhou Y, Wang L, Ban X, Zeng T, Zhu Y, Li M, Guan XY and Li Y: DHRS2 inhibits cell growth and motility in esophageal squamous cell carcinoma. Oncogene 37: 1086-1094, 2018.
48. Wessels D, Murray J, Jung G, Hammer JA III and Soll DR: Myosin IB null mutants of Dictyostelium exhibit abnormalities in motility. Cell Motil Cytoskeleton 20: 301-315, 1991.
49. Ohmura G, Tsujikawa T, Yaguchi T, Kawamura N, Mikami S, Sugiyama J, Nakamura K, Kobayashi A, Iwata T, Nakano H, *et al*: Aberrant Myosin 1b Expression Promotes Cell Migration and Lymph Node Metastasis of HNSCC. Mol Cancer Res 13: 721-731, 2015.
50. Elowe S: Bub1 and BubR1: At the interface between chromosome attachment and the spindle checkpoint. Mol Cell Biol 31: 3085-3093, 2011.
51. Athanasoula KC, Gogas H, Polonifi K, Vaiopoulos AG, Polyzos A and Mantzourani M: Survivin beyond physiology: Orchestration of multistep carcinogenesis and therapeutic potentials. Cancer Lett 347: 175-182, 2014.
52. Aytes A, Mitrofanova A, Lefebvre C, Alvarez MJ, Castillo-Martin M, Zheng T, Eastham JA, Gopalan A, Pienta KJ, Shen MM, *et al*: Cross-species regulatory network analysis identifies a synergistic interaction between FOXM1 and CENPF that drives prostate cancer malignancy. Cancer Cell 25: 638-651, 2014.
53. Asghar U, Witkiewicz AK, Turner NC and Knudsen ES: The history and future of targeting cyclin-dependent kinases in cancer therapy. Nat Rev Drug Discov 14: 130-146, 2015.
54. Chen T, Sun Y, Ji P, Kopetz S and Zhang W: Topoisomerase IIα in chromosome instability and personalized cancer therapy. Oncogene 34: 4019-4031, 2015.